

## Supplementary Information

### **Abnormal self-discharge in lithium-ion batteries**

Won Mo Seong<sup>a</sup>, Kyu-Young Park<sup>a</sup>, Myeong Hwan Lee<sup>a</sup>, Sehwan Moon<sup>a</sup>, Kyungbae Oh<sup>ab</sup>, Hyeokjun Park<sup>ab</sup>, Sechan Lee<sup>a</sup>, and Kisuk Kang<sup>ab\*</sup>

<sup>a</sup>Department of Materials Science and Engineering, Research Institute of Advanced Materials (RIAM), Seoul National University, Seoul 08826, Republic of Korea

<sup>b</sup>Center for Nanoparticle Research, Institute for Basic Science (IBS), Seoul 08826, Republic of Korea

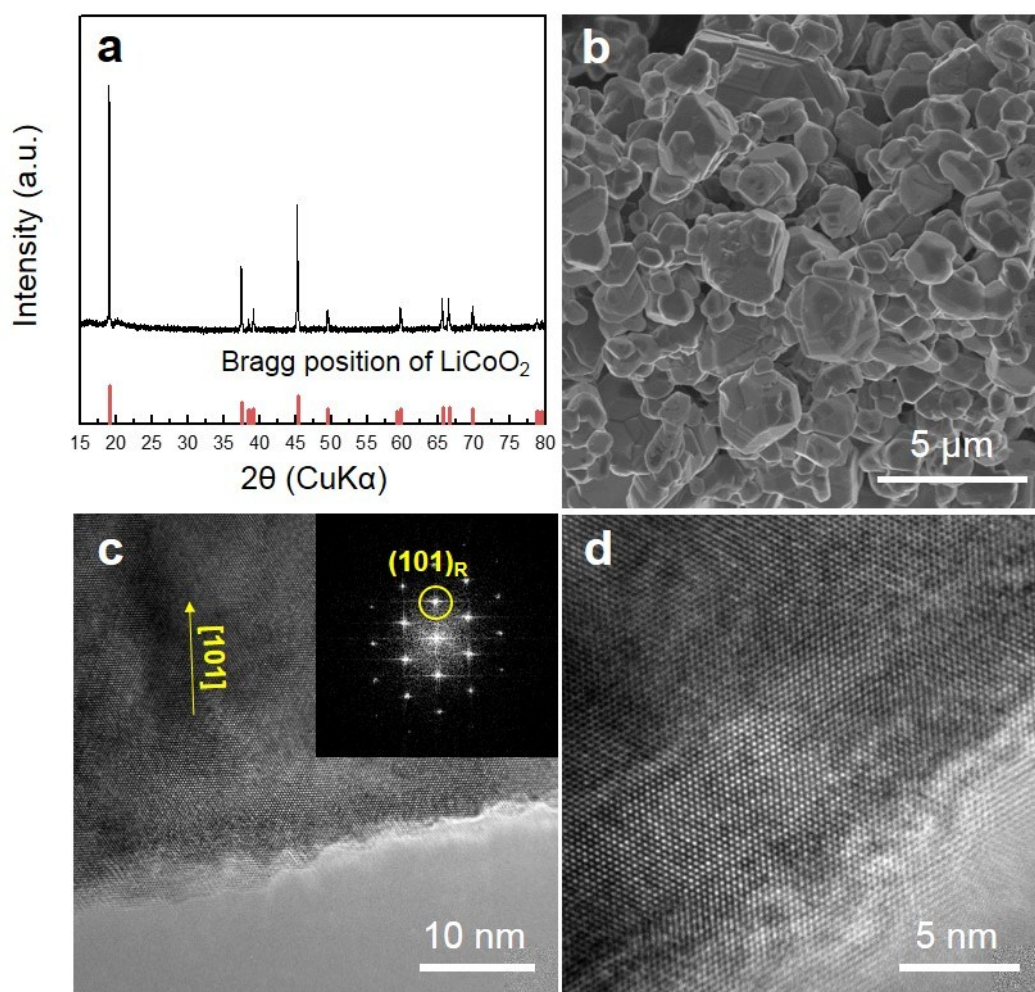


**Figure S1.** (a) XRD pattern, (b) SEM image, (c) and (d) high-resolution TEM (HRTEM) lattice image of LiCoO<sub>2</sub> powder. The inset in (c) shows the fast Fourier transformation calculated from the entire image.

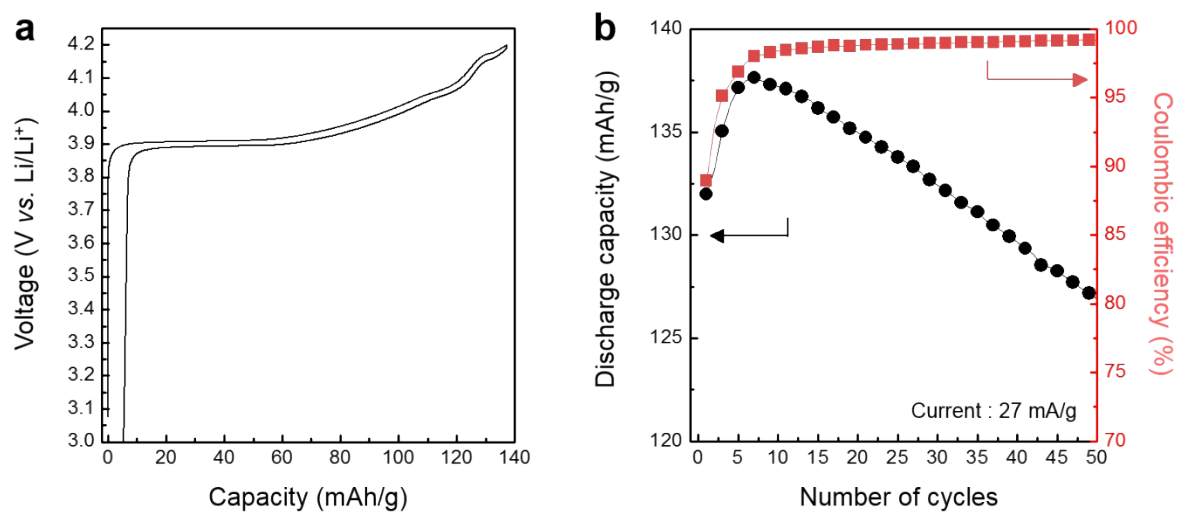


**Figure S2.** (a) Charge-discharge profile at sixth cycle and (b) cycle stability of Li/LiCoO<sub>2</sub> cell.

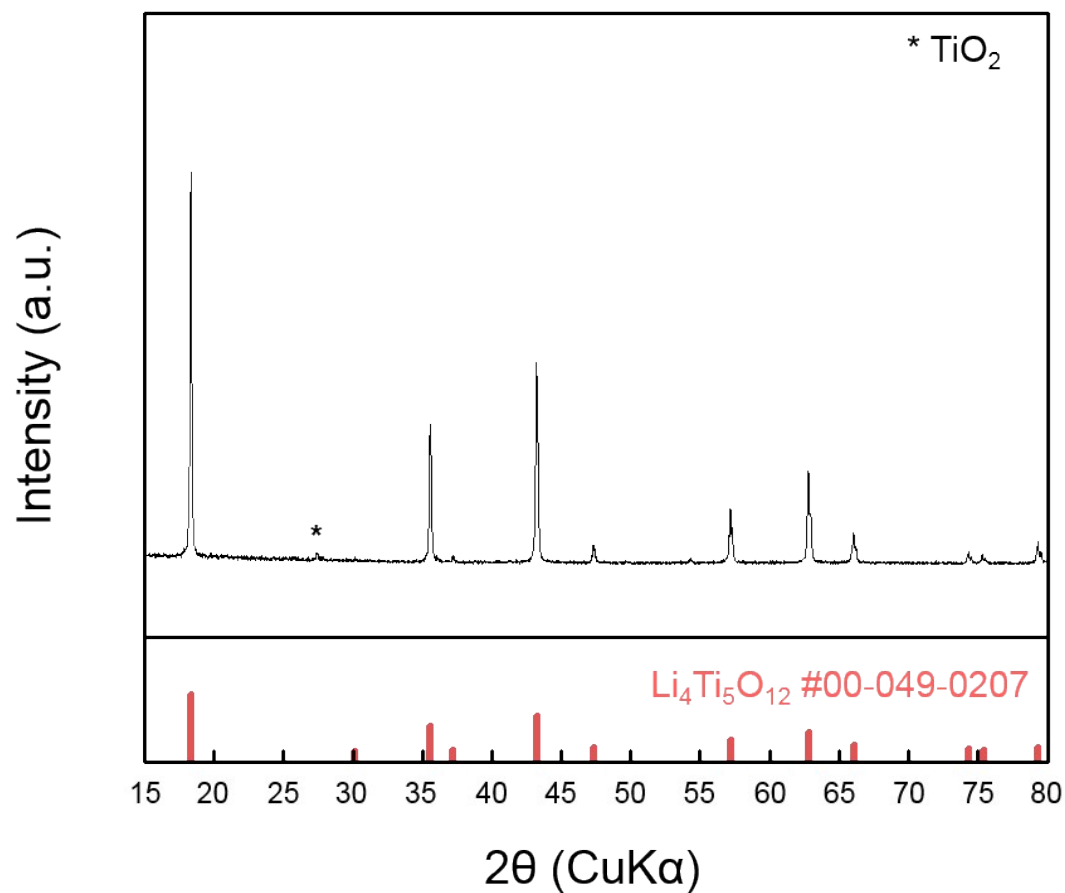


**Figure S3.** X-ray diffraction pattern of synthesized  $\text{Li}_4\text{Ti}_5\text{O}_{12}$  powder.

To obtain the desired material, stoichiometric quantities of  $\text{Li}_2\text{CO}_3$  (98% Aldrich) and  $\text{TiO}_2$  (99% Aldrich) were mixed using high-energy ball milling (Pulverisette 5, FRITSCH) at 400 rpm for 12 h, and the mixture was calcined at 850 °C for 6 h in air. The resulting powder was confirmed to be spinel  $\text{Li}_4\text{Ti}_5\text{O}_{12}$  with Fd-3m space group based on XRD measurements.

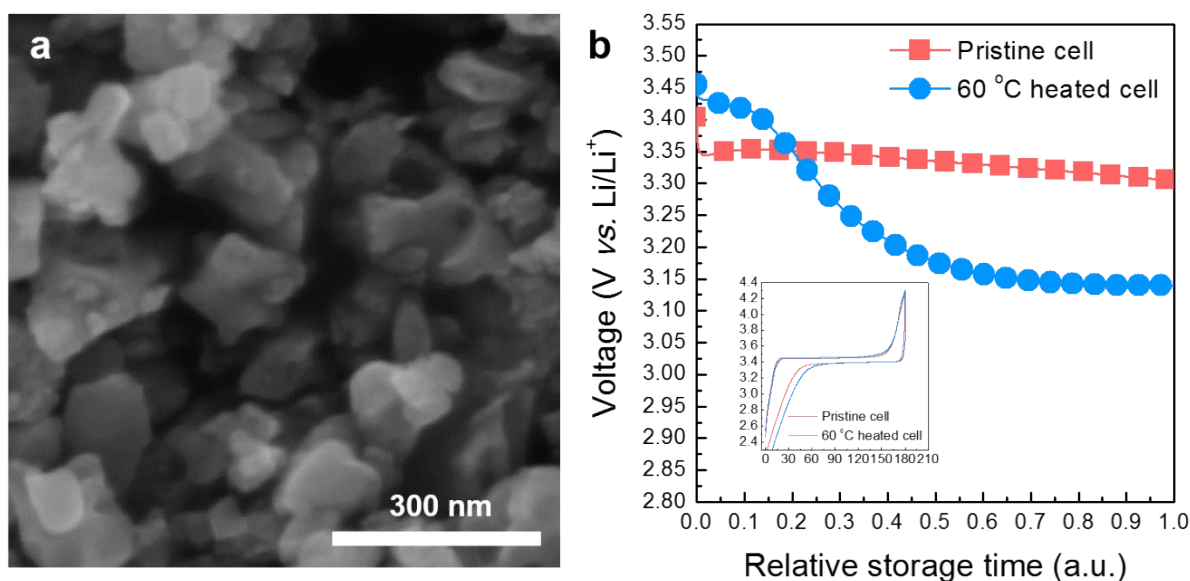


**Figure S4.** (a) SEM images of synthesized  $\text{LiFePO}_4$  particle, respectively. (b) Representative voltage decay curve of  $\text{Li}_x\text{FePO}_4$  and  $\text{Li}(\text{Ni}_{0.6}\text{Co}_{0.2}\text{Mn}_{0.2})\text{O}_2$  cathode charged to SOC 20, respectively, with/without 60 °C thermal history. Inset figure shows the representative voltage profile of  $\text{Li/LiFePO}_4$  cell. Current rate was set to 17 mA/g.

In the synthesis of  $\text{LiFePO}_4$  (LFP), a stoichiometric amount of  $\text{Li}_2\text{CO}_3$ ,  $\text{FeC}_2\text{O}_4 \cdot \text{H}_2\text{O}$  and  $(\text{NH}_4)_2\text{HPO}_4$  were mixed by wet ball-milling process in acetone for 24 hours, dried in vacuum, calcined at 350 °C for 10 hours, pelletized and heated at 600 °C again for 10 hours in Ar atmosphere<sup>1</sup>. The pristine material was used without additional surface treatment. The morphology of the material is provided in **Figure S4a**, which is consistent with previous literatures<sup>1,2</sup>. For the LFP sample, the electrodes were fabricated in almost same way with that for  $\text{LiCoO}_2$  electrodes; the mixture of LFP, polyvinylidene fluoride (PVDF) binder, and super-P carbon with weight ratio of 7:1:2 was dissolved in N-Methyl-2-pyrrolidone (NMP) solvent, then the slurry was applied onto Al foil by doctor-blade method. The electrodes were dried at room temperature for overnight before use. The coin-cells employing the LFP cathode, 1 M  $\text{LiPF}_6$  in EC/DMC (1:1 v/v) electrolyte, GF/F glass fiber separator and Li metal anode were assembled and stored at 60 °C for 10 hours in identical protocols to the case of  $\text{LiCoO}_2$  cells. After the short-term thermal history, the cell was charged into SOC 20 states, and their behaviors of voltage decay were carefully monitored in comparison to the one without the thermal history. Since the LFP undergoes the

two-phase reaction with a flat voltage ( $\sim 3.4$  V vs.  $\text{Li/Li}^+$ ), a significant deviation from 3.4 V in the OCV would imply the self-discharge. In fact, we observed that the self-discharge is obviously accelerated in the case of LFP with the short-term thermal history as shown in **Figure S4b**. While the LFP electrode without thermal history (denoted as ‘pristine cell’) maintains its characteristic 3.4 V for the extended time (10 days), the one with the thermal history (denoted as ‘60°C heated cell’) displays the rapid voltage drop after 3 days. It clearly demonstrates that the LFP electrode undergoes the serious self-discharge once the thermal history is recorded.

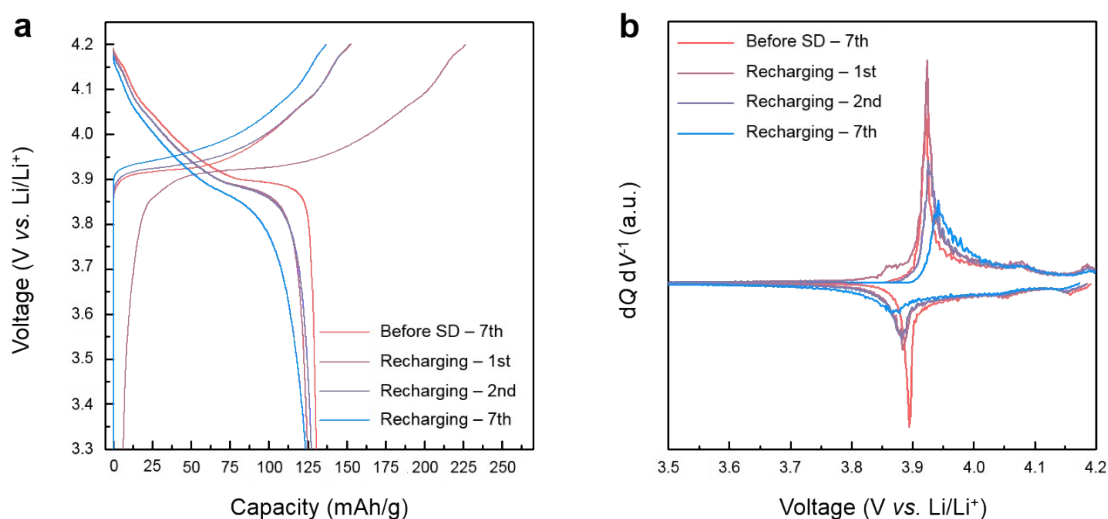


**Figure S5.** (a) Voltage profiles and (b)  $dQ/dV$  plots from (a) of self-discharged  $\text{Li}_x\text{CoO}_2$  for which a thermal history at 60 °C was written obtained by recharging it with a current of 27 mA/g. The voltage profile was monitored until the 7th cycle, and the representative results are compared with that before the  $\text{Li}_x\text{CoO}_2$  was self-discharged (marked as ‘Before SD (self-discharge)’).

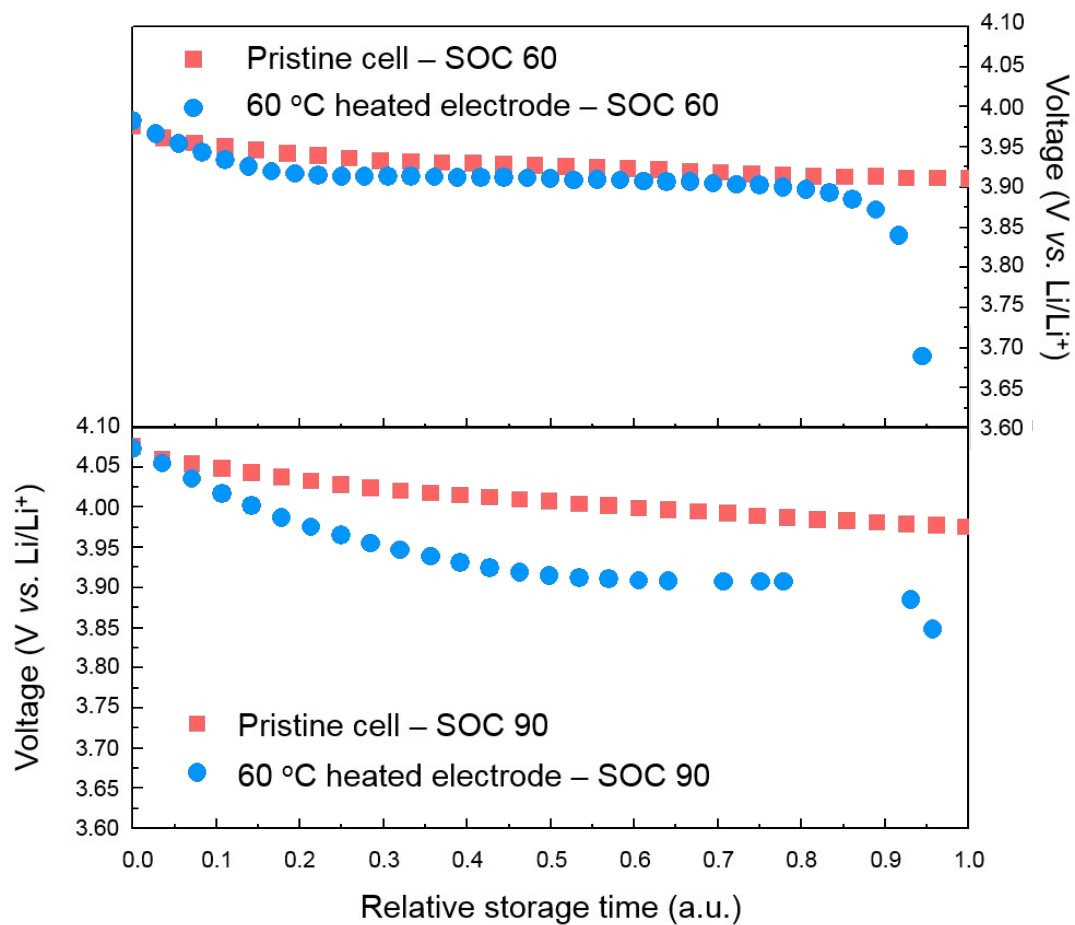


**Figure S6.** Voltage decay curve of LiCoO<sub>2</sub> cathode with thermal history at 60 °C at various SOC (SOC 60 and 90). All the measurements were performed at 25 °C. In each case, the voltage decay behavior was universally observed upon storage at 60 °C.

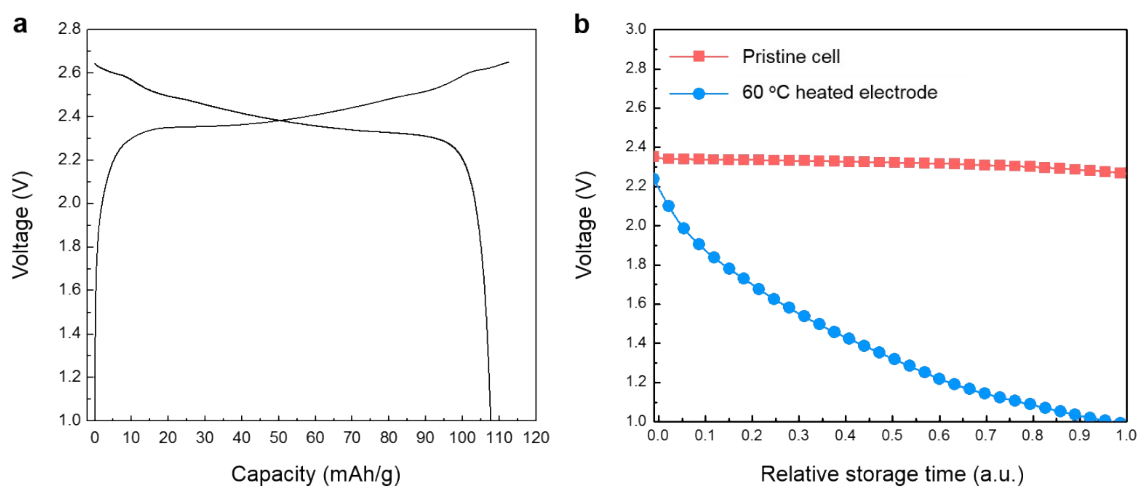


**Figure S7.** (a) Typical charge/discharge profile of a full cell using a  $\text{Li}_x\text{CoO}_2$  cathode and  $\text{Li}_{4+x}\text{Ti}_5\text{O}_{12}$  anode. (b) Decay of OCV for a cell exposed to 60 °C heat treatment. The cathode was soaked in electrolyte solution at 60 °C.



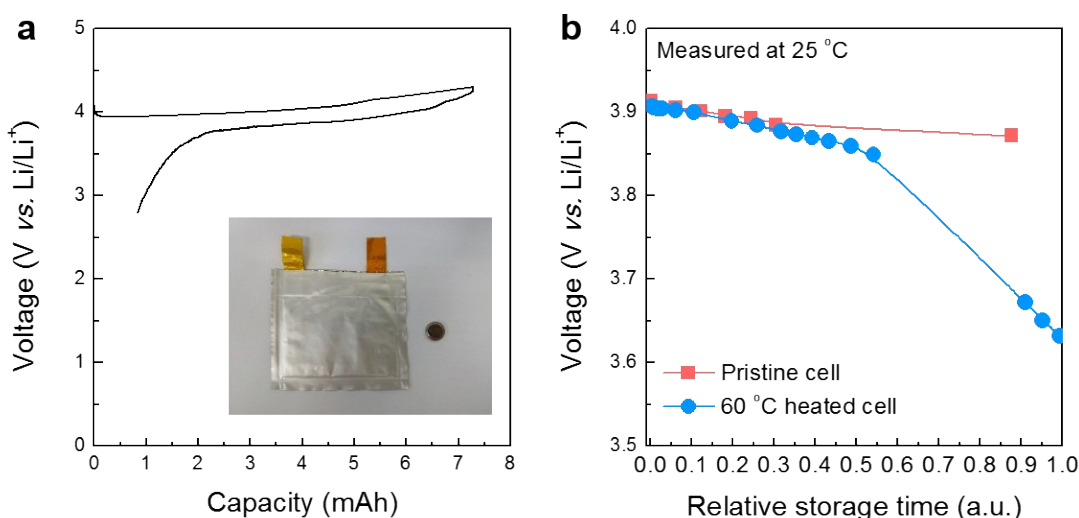


**Figure S8.** (a) Representative electrochemical voltage profile of Li/LiCoO<sub>2</sub> pouch-type cell. Current density for charge and discharge was set to 1 mA. Inset photograph shows the relative size of the pouch (left: 10 cm x 10 cm) compared with the conventional 2032 coin-type cell (right). The pouch-type cell was fabricated using 2 cm x 7 cm rectangular LiCoO<sub>2</sub> cathode, lithium metal anode, 1 M LiPF<sub>6</sub> in EC/DMC (1:1 v/v) and Celgard 2400 separator. (b) The probe of the voltage decay as a function of time for the pouch-cell containing Li<sub>x</sub>CoO<sub>2</sub> cathode with/without 60 °C thermal history. The open-circuit-voltages of the two cells were monitored for 5 days.

The fabricated cell is shown in the inset (left) of **Figure S8a**, in comparison to the original 2032 coin-type cell (right). The electrochemical operation of the cell showed the characteristic charge/discharge profile of LiCoO<sub>2</sub> cathode at the current of 1 mA in the voltage range of 2.8-4.3 V (vs. Li/Li<sup>+</sup>) as shown in **Figure S8a**. For this fabricated pouch-type cell, we performed the same self-discharge test as in the original coin cell with or without thermal history. **Figure S8b** clearly confirms that the accelerated self-discharge induced from a short-term thermal exposure is observed in the practically used pouch-type cell. Compared with the cell without a thermal history (indicated as ‘pristine cell’ in the graph), the open-circuit-voltage of the pouch-cell suddenly drops after a few days of storage below 3.6 V when 60 °C of thermal history had been recorded (indicated as ‘60 °C heated cell’ in the graph). Note that it is an even more dramatic difference arising from the thermal history than the case observed for the coin cell. While it can be partly attributed to the non-optimized pouch-type cell configuration here, it implies that the surface parasitic reaction that causes the self-discharge can be more sensitively expedited with the un-optimization of cells.

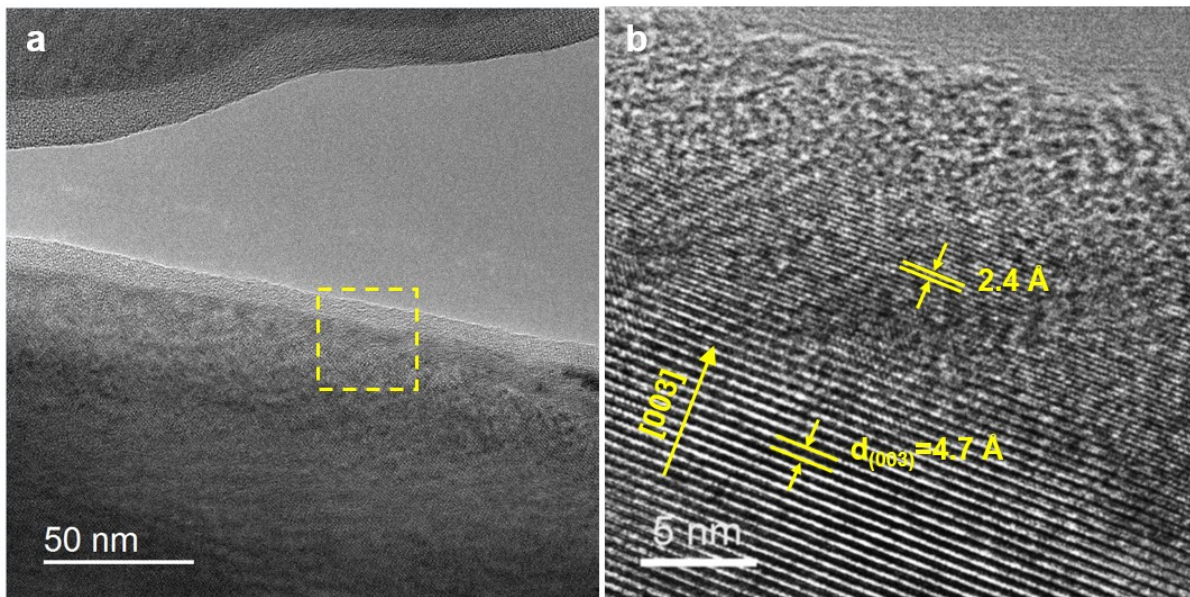


**Figure S9.** TEM images of surface of  $\text{Li}_x\text{CoO}_2$  without heating: (a) low-magnification image and (b) high-magnification image of region outlined by yellow dashed square in (a).

The 5-nm-thick crystalline region adjacent to the amorphous surface layer has a d-spacing of 2.4 Å, unlike that of the bulk region of 4.7 Å, which likely corresponds to the reduction of  $\text{Li}_x\text{CoO}_2$  due to electrolyte oxidation, as previously observed by Ogumi *et al.*<sup>3</sup>. This electrolyte oxidation may cause the extraction of lithium and induce the transformation of the  $\text{LiCoO}_2$  at the surface to  $\text{Co}_3\text{O}_4$  or other species *via* reduction.

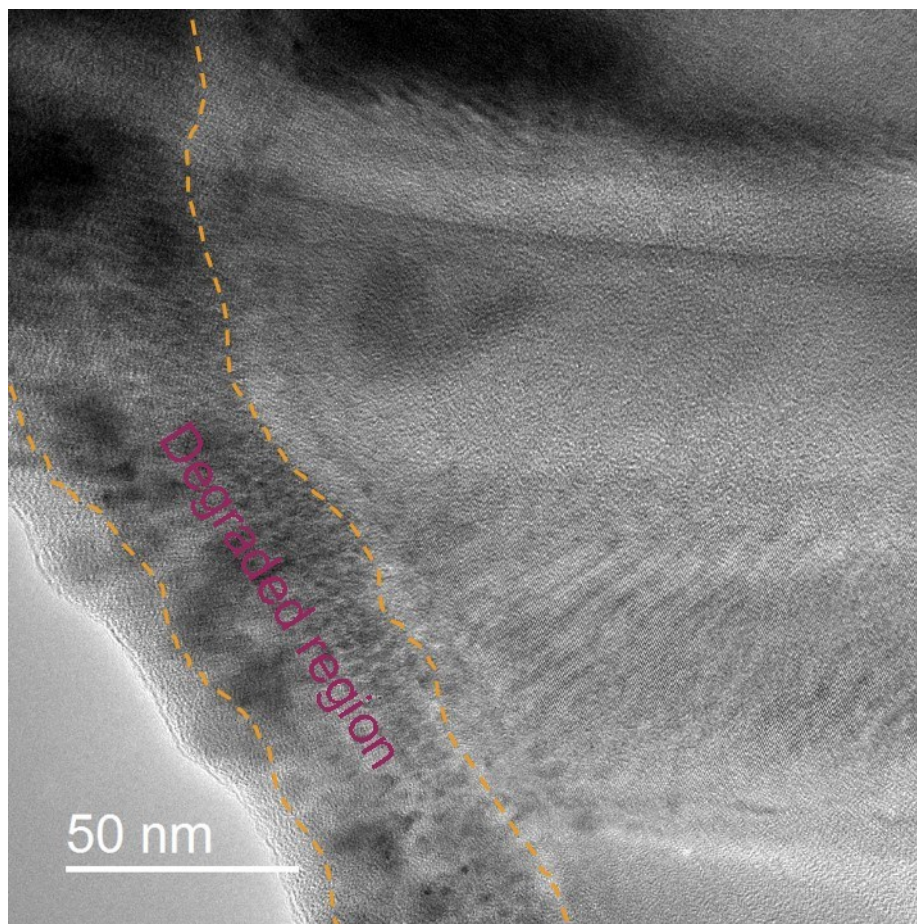


**Figure S10.** Low-magnification TEM image of  $\text{Li}_x\text{CoO}_2$  obtained directly after charge to SOC 20 for which a thermal history of 60 °C was recorded.

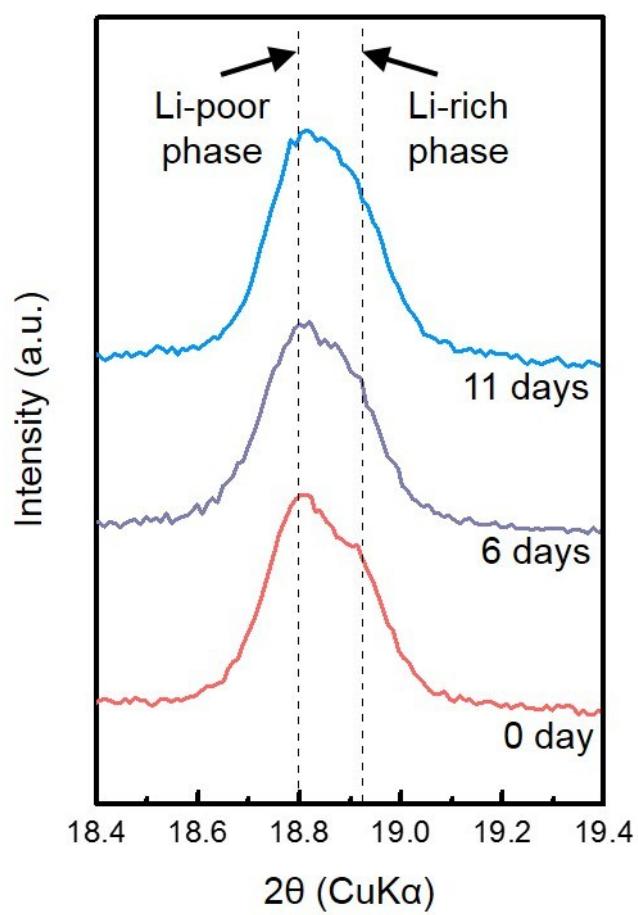


**Figure S11.** Trace of XRD patterns of charged  $\text{Li}_x\text{CoO}_2$  (SOC 20) electrode without thermal history.

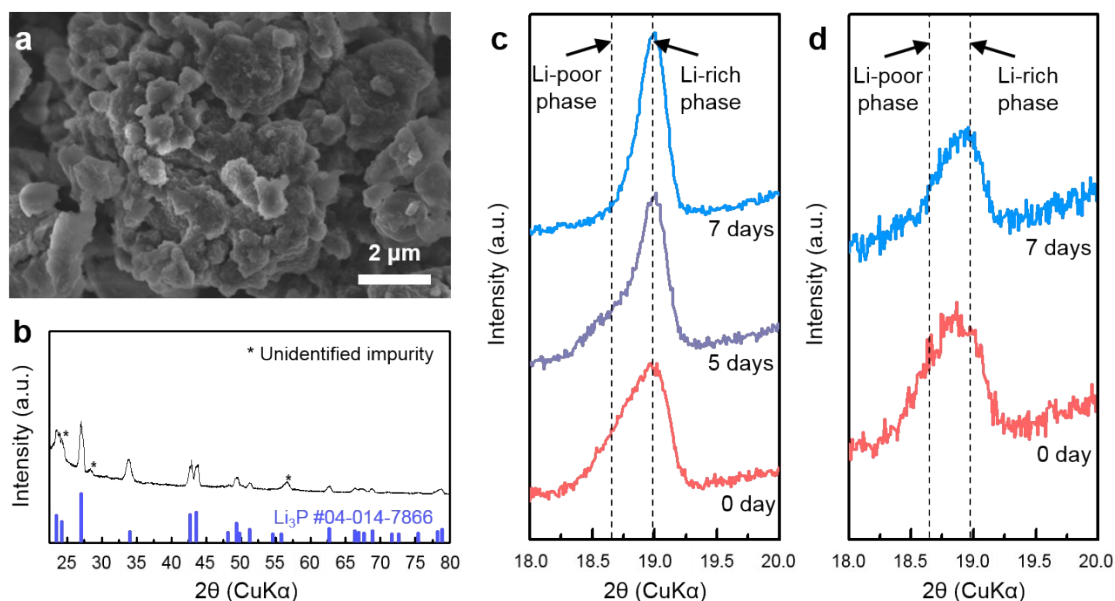


**Figure S12.** (a) SEM image and (b) XRD pattern of synthesized  $\text{Li}_3\text{P}$  powder. Traces of XRD patterns of delithiated  $\text{Li}_{0.9}\text{CoO}_2$  powder (c) mixed with  $\text{Li}_3\text{P}$  powder or (d) not mixed with  $\text{Li}_3\text{P}$  powder during storage in an argon atmosphere.

To synthesize  $\text{Li}_3\text{P}$ , we used a previously reported method<sup>4</sup>. Li metal and red phosphorus powder were mixed and heated at 200 °C for 5 h, and the surrounding environment was further increased to 400 °C and maintained at this temperature for 5 h. The resulting compound was ground using a mortar and calcined again at 400 °C for 5 h. The entire procedure, including the calcination and grinding, was conducted in an argon atmosphere. As observed in the SEM image in **Figure S12a**, the average size of the  $\text{Li}_3\text{P}$  particles was  $\sim 1\ \mu\text{m}$ , which is smaller than that of  $\text{LiCoO}_2$  (see **Figure S1b**). This finding indicates that the contact of  $\text{Li}_3\text{P}$  and  $\text{LiCoO}_2$  is intact when they are mixed together. The XRD pattern of the resulting powder in **Figure S12b** indicates the presence of the  $\text{Li}_3\text{P}$  phase as the majority phase and other unidentified impurity as the minority phase. The  $\text{Li}_3\text{P}$  powder was mixed with charged  $\text{Li}_{0.9}\text{CoO}_2$  powder retrieved from the charged Li/ $\text{LiCoO}_2$  coin cell (half of the retrieved powder was mixed with  $\text{Li}_3\text{P}$  powder at a weight ratio of 10:1). The XRD pattern of this mixture (which was stored

in an argon atmosphere) was monitored for 7 days and compared with that from only  $\text{Li}_{0.9}\text{CoO}_2$ , which was obtained from the other half of the  $\text{Li}_{0.9}\text{CoO}_2$  powder retrieved from the charged coin cell.



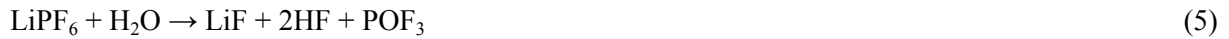
**Supplementary Note 1** (Discussion on the formation of phosphide impurities on the surface of  $\text{Li}_x\text{CoO}_2$  by the side reaction with electrolyte). It is well known that the thermal stability  $\text{LiPF}_6$  salt is relatively poor, and its decomposition starts from 107 °C<sup>4</sup>. Generally, the decomposition proceeds as shown by the following equations<sup>5-7</sup>:



When there is a trace amount of water in the electrolyte, HF is formed and triggers series of reactions shown below<sup>6,7</sup>:



Meanwhile, it is also known that a trace amount of water in electrolyte can react with salt itself to form HF<sup>5</sup>:



It was suggested that several forms of fluorinated phosphoric acids can be formed, which led to formation of phosphoric acid<sup>8</sup>:



Because of continuous generation of water as shown in equation (3) and (4), only small trace of water is sufficient to induce these reactions. Previous studies have suggested the role of phosphoric acid acting as phosphorus source for the formation of phosphide when it is in chemical contact with metal sources in highly oxidative conditions such as at high temperature<sup>9,10</sup>. We believe that this scenario is also applicable in the case of the surface of  $\text{LiCoO}_2$  by the thermal history, where the phosphoric acid leaches out the lithium from  $\text{LiCoO}_2$  forming the  $\text{Li}_3\text{P}$ . Therefore, only short exposure of electrolyte/electrode interface to 60 °C or 80 °C is enough to generate small amount of phosphide impurities to complete the chemical lithiation of  $\text{Li}_x\text{CoO}_2$  during abnormal self-discharge.

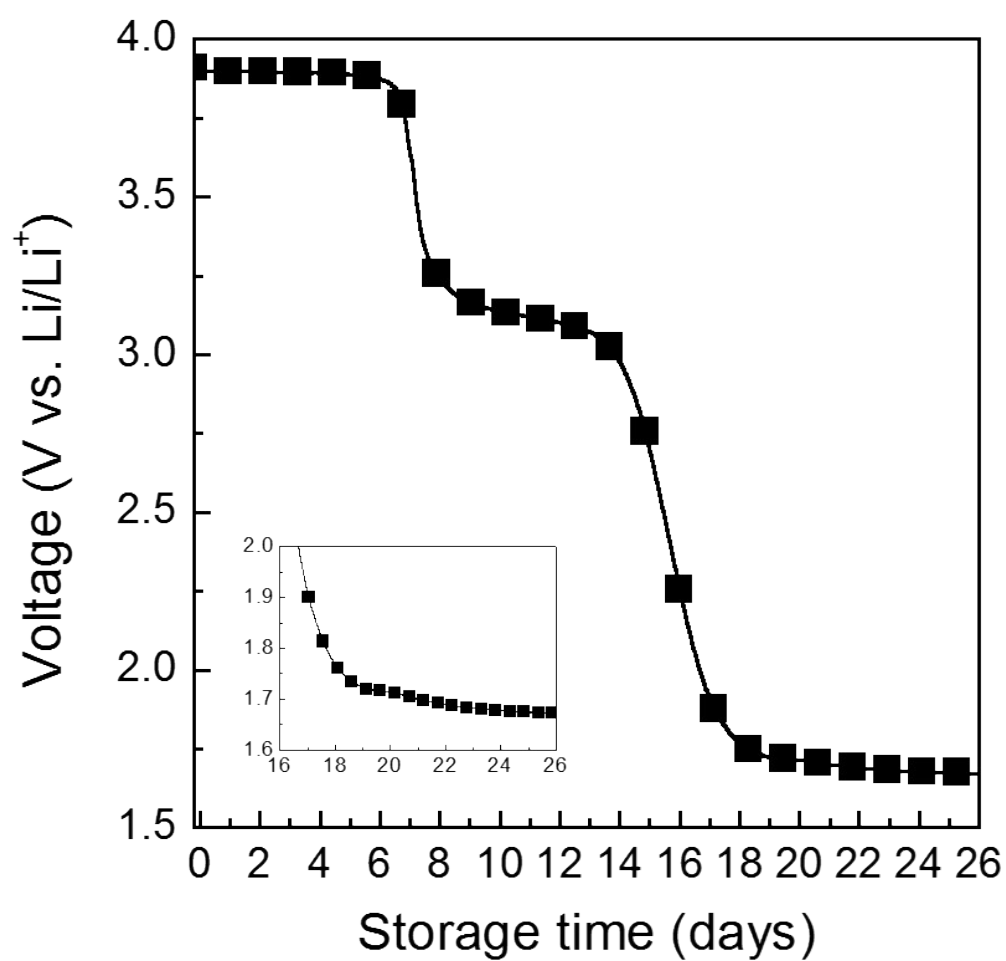


**Figure S13.** Change of open-circuit voltage of Li/LiCoO<sub>2</sub> cell with thermal history during storage which is allowed to decrease under 3.0 V. Inset shows the same figure magnified at the region nearby ~1.7 V.



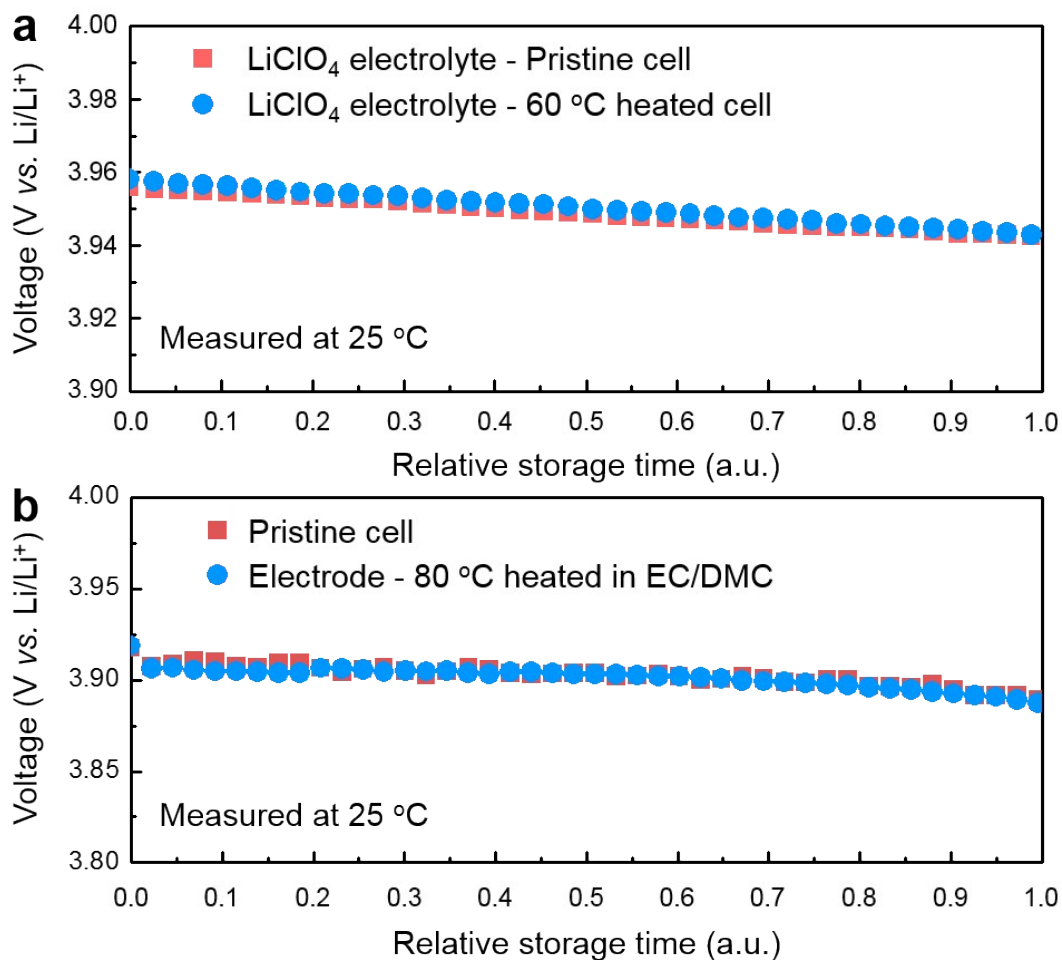


**Figure S14.** (a) Comparison of self-discharge rate of bare LiCoO<sub>2</sub> and LiCoO<sub>2</sub> with 60 °C thermal history using electrolyte of 1 M LiClO<sub>4</sub> in EC/DMC (1:1 v/v). (b) Comparison of self-discharge rate of bare LiCoO<sub>2</sub> and LiCoO<sub>2</sub> with thermal history consisting of soaking the cathode electrode in EC/DMC (1:1 v/v) solvent without salt at 80 °C. The self-discharge rate in (b) was measured using 1 M LiPF<sub>6</sub> in EC/DMC (1:1 v/v) electrolyte.

**Supplementary Note 2 (Quantitative estimation of the thickness of  $\text{Li}_3\text{P}$  film required for the chemical discharge of charged  $\text{Li}_x\text{CoO}_2$ ).** Based on the SEM observation in Figure S1b, we assumed that the shape of the  $\text{Li}_x\text{CoO}_2$  particle was a perfect sphere with an average diameter of 2  $\mu\text{m}$ . This assumption renders the radius of the sphere 1  $\mu\text{m}$ , simplifying our calculation. Here, we suggest the situation that lithium inserted into the  $\text{Li}_x\text{CoO}_2$  sphere is provided by the surface film composed of only  $\text{Li}_3\text{P}$ . Using densities of 5.06 and 1.44  $\text{g/cm}^3$  and molecular masses of 97.87 and 51.80  $\text{g/mol}$  for  $\text{LiCoO}_2$  and  $\text{Li}_3\text{P}^{11,12}$ , respectively, we calculated the amounts of these materials per cubic centimeter to be 52 and 28 mmol, respectively. Based on our suggestion for the route of self-discharge expressed in Equation [1] in the main text,  $\text{Li}_3\text{P}$  can be considered to provide 2 Li per unit chemical formula. Therefore,  $\text{Li}_x\text{CoO}_2$  occupies 52 mmol of lithium sites and  $\text{Li}_3\text{P}$  provides 56 mmol of lithium per cubic centimeter. Thus, for the same volume,  $\text{Li}_3\text{P}$  has  $\sim 1.08$  times the number of lithium sites of those in  $\text{Li}_x\text{CoO}_2$ . In addition, for this simple calculation, we make the assumption that the size of the  $\text{Li}_x\text{CoO}_2$  sphere does not change even when the thermal history transforms its surface into a  $\text{Li}_3\text{P}$  thin film, as shown in **Figure S15**.

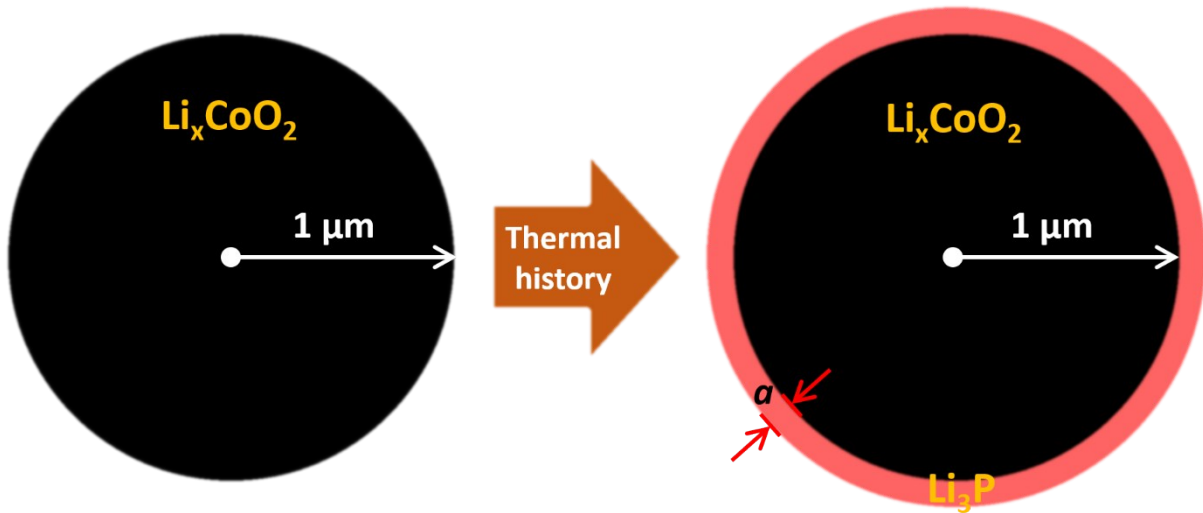


**Figure S15.** Simplified model for calculation of required  $\text{Li}_3\text{P}$  film thickness ( $a$  in the sphere right side) for chemical lithiation of charged sphere  $\text{Li}_x\text{CoO}_2$  with radius of 1  $\mu\text{m}$ .

For the  $\text{Li}_3\text{P}$  film to fully lithiate the charged  $\text{Li}_x\text{CoO}_2$ , the number of lithium sites provided by the  $\text{Li}_3\text{P}$  film should be more than that in the  $\text{Li}_x\text{CoO}_2$  bulk. Therefore, we can calculate the minimum number of lithium sites in the  $\text{Li}_3\text{P}$  film for chemical lithiation of  $\text{Li}_x\text{CoO}_2$  as follows:

$$(\text{Number of Li sites in unit Li}_x\text{CoO}_2) = (\text{Number of Li sites provided by unit Li}_3\text{P})$$

Because we already calculated that the number of lithium sites per unit volume in  $\text{Li}_3\text{P}$  is 1.08 times that in  $\text{Li}_x\text{CoO}_2$ , the above equation can be written as

$$(1 - x) \times (\text{Volume of Li}_x\text{CoO}_2) = 1.08 \times (\text{Volume of Li}_3\text{P}).$$

Thus, the thickness of the  $\text{Li}_3\text{P}$  film,  $a$ , can be calculated as follows:

$$(1 - x) \times \frac{4}{3} \times \pi \times (1 \mu\text{m})^3 = 1.08 \times \frac{4}{3} \times \pi \times ((a + 1)\mu\text{m})^3 - (1 \mu\text{m})^3).$$

In each SOC, we can input the corresponding  $x$  and find  $a$  by solving the cubic equation above. Thus, when  $\text{Li}_x\text{CoO}_2$  is charged to  $x=0.9$ ,  $a$  is calculated to be  $\sim 0.030$ , corresponding to a thickness of only 30 nm. Even when  $\text{Li}_x\text{CoO}_2$  is charged to  $x=0.5$ , representing the broadly known limit of charge for reversible operation of a secondary battery composed of this material,  $a$  is calculated to be  $\sim 0.135$ , corresponding to a thickness of 135 nm. These results strongly support the notion that even a slight detrimental reaction between  $\text{Li}_x\text{CoO}_2$  and the electrolyte during a short period of heating can induce severe acceleration of the self-discharge.

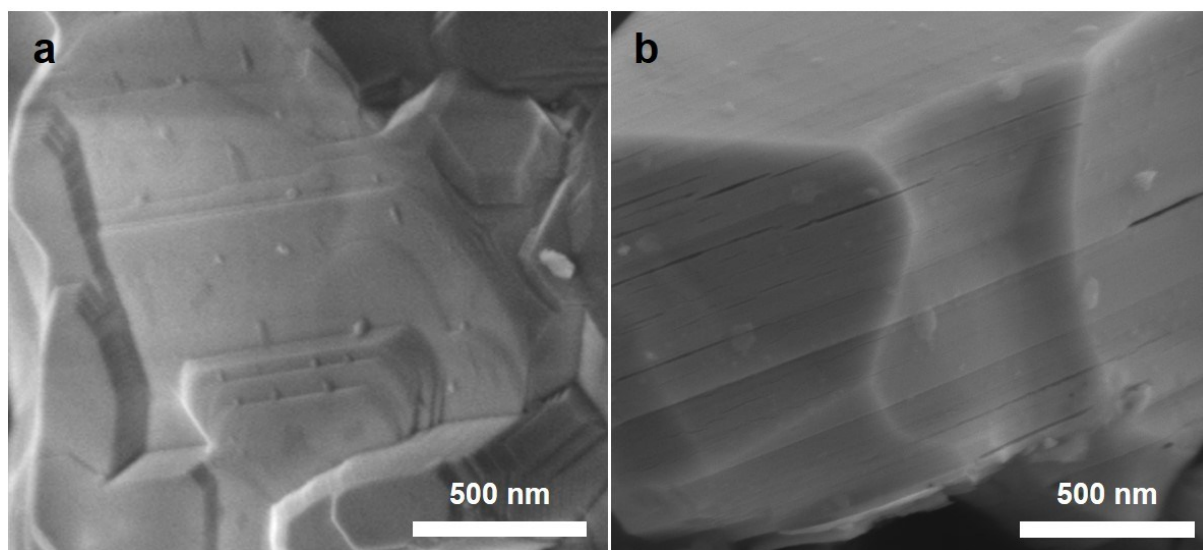


**Figure S16.** SEM image of surface of (a) pristine LiCoO<sub>2</sub> and (b) LiCoO<sub>2</sub> cycled at 4.8 V-cut off for 50 cycles.

## Reference

1. K. –Y. Park, I. Park, H. Kim, G. Yoon, H. Gwon, Y. Cho, Y. S. Yun, J. –J. Kim, S. Lee, D. Ahn, Y. Kim, H. Kim, I. Hwang, W. –S. Yoon and K. Kang, *Energy Environ. Sci.*, 2016, **9**, 2902.2915.
2. H. Liu, F. C. Strobridge, O. J. Borkiewicz, K. M. Wiaderek, K. W. Chapman, P. J. Chupas, C. P. Grey, *Science*, 2014, **344**, 1252817.
3. D. Takamatsu, Y. Koyama, Y. Orikasa, S. Mori, T. Nakatsutsumi, T. Hirano, H. Tanida, H. Arai, Y. Uchimoto and Z. Ogumi, *Angew. Chem. Int. Ed.*, 2012, **51**, 11597-11601.
4. G. A. Nazri, R. A. Conell and C. Julien, *Solid State Ionics*, 1996, **86**, 99-105.
5. Y. Gu, D. Chen and X. Jiao, *J. Phys. Chem. B*, 2005, **109**, 17901-17906.
6. Y. Takanashi, Y. Orikasa, M. Mogi, M. Oishi, H. Murayama, K. Sato, H. Yamashige, D. Takamatsu, T. Fujimoto, H. Tanida, H. Arai, T. Ohta, E. Matsubara, Y. Uchimoto and Z. Ogumi, *J. Power Sources*, 2011, **196**, 10679-10685.
7. H. Yang, G. V. Zhuang and P. N. Ross Jr., *J. Power Sources*, 2006, **161**, 573-579.
8. P. Andersson, P. Blomqvist, A. Loren and F. Larsson, *Fire Mater.*, 2016, **40**, 999-1015.
9. C. H. Choi, S. H. Park and S. I. Woo, *J. Mater. Chem.*, 2012, **22**, 12107-12115.
10. M. C. Lopez, G. F. Ortiz and J. L. Tirado, *J. Electrochem. Soc.*, 2012, **159**, A1253-A1261.
11. *LiCoO<sub>2</sub> Crystal Structure: Datasheet from "PAULING FILE Multinaries Edition – 2012" in SpringerMaterials* ([http://materials.springer.com/isp/crystallographic/docs/sd\\_0554601](http://materials.springer.com/isp/crystallographic/docs/sd_0554601)), Springer-Verlag Berlin Heidelberg & Material Phases Data System (MPDS), Switzerland & National Institute for Materials Science (NIMS), Japan.
12. *Li<sub>3</sub>P Crystal Structure: Datasheet from "PAULING FILE Multinaries Edition – 2012" in SpringerMaterials* ([http://materials.springer.com/isp/crystallographic/docs/sd\\_0458524](http://materials.springer.com/isp/crystallographic/docs/sd_0458524)), Springer-Verlag Berlin Heidelberg & Material Phases Data System (MPDS), Switzerland & National Institute for Materials Science (NIMS), Japan.